The impact of deforestation on orographic cloud formation in a complex tropical environment

U.S. Nair[1], D.K. Ray[2], R.O. Lawton[3], R.M. Welch[2], and R.A. Pielke Sr.[4], J. Calvo [5]

[1] Earth Science System Center
National Space Science Technology Center
University of Alabama in Huntsville
Huntsville, AL 35806

[2] Department of Atmospheric Science
National Space Science Technology Center
University of Alabama in Huntsville
Huntsville, AL 35806

[3] Department of Biological Sciences
National Space Science Technology Center
University of Alabama in Huntsville
Huntsville, AL 35899

[4]Department of Atmospheric Science
Colorado State University
Fort Collins, CO 80523-1371

[5] Instituto Tecnologico De Costa Rica

Submitted to:

Mountains in the Mist, Proceedings of the 2nd International Symposium on Tropical Montane Cloud Forests

May 12, 2005

ABSTRACT

Ecological changes observed at cloud forests in Monteverde, Costa Rica, including disappearance of anuran populations and expansion of bird and bat ranges to higher elevations has been linked to an increasing trend in dry season mist free days. Prior studies suggest that the increasing trend in dry season mist free days may be influence by both large scale climate change processes and also regional scale changes in land use. Preliminary investigations exploring the impact of land use on cloud formation indicated that drying and warming of boundary layer air in response to deforestation leads to increased cloud base heights. In the present study, numerical model experiments utilizing realistic land use scenarios and atmospheric conditions are used to further explore the impact of land use on orographic cloud formation.

The Regional Atmospheric Modeling System (RAMS) is used to simulate orographic cloud formation during the time period of 1-14 March, 2003 in the Monteverde region for pristine, current and future land use scenarios. These simulations are initiated from the same atmospheric conditions and are subject to similar lateral boundary conditions. Comparisons against observations show that RAMS realistically simulate the nature of orographic cloud formation and boundary layer thermodynamics. Numerical simulations show that deforestation in the lowlands and premontane areas results in an increase in average cloud base heights and a consequent decrease in the areal extent of montane forests immersed in clouds. In the current and future land use scenarios, an increase in Bowen ratio and warmer, drier air is found over lowlands and premontane areas. The simulated differences in cloud formation and air mass

thermodynamics are positively correlated to the amount of deforestation in the lowland and premontane regions.

1 Introduction

Analysis of meteorological observations at Monteverde, Costa Rica, indicates a pattern of increase in dry season mist free days since early 1970s (Pounds et al., 1999). Since the dry season input of moisture from orographic clouds is crucial for the tropical montane cloud forest ecosystem the increase in mist free days may be responsible for the ecological changes observed in this region. Coinciding with the increase of mist free days, observations document collapses of anuran populations and expansion of bird and bat ranges to higher elevations (Pounds et al., 1999; LaVal 2004). The diurnal changes in temperature during the same time period show a decreasing trend, implying increase of cloudiness, particularly nocturnal cloudiness, in the Monteverde region. Under these conditions decrease in dry season mist frequency implies an increase in cloud base height.

Recent studies have explored potential processes that might contribute to elevation of orographic cloud base height in Monteverde and montane sites in other parts of the world that harbor cloud forest ecosystems (Still et al., 1999; Lawton et al., 2001; Nair et al., 2003). These studies suggest that sudden warming of tropical oceans in the mid 1970s (Pounds et al., 1999), climate change forced by increasing atmospheric carbon dioxide (Still et al., 1999) and land use change (Lawton et al., 2001; Nair et al., 2003) could all potentially contribute to increased orographic cloud base heights.

Still et al. (1999) used Global Circulation Model (GCM) simulations of climate with current and doubled atmospheric carbon dioxide concentrations to examine the effect of climate change on cloud base heights at various high altitude locations around the world. Using height of relative humidity surfaces in these simulations as a proxy for cloud base height, Still et al. (1999) calculated increases in cloud base heights of up to 300m in response to doubled atmospheric carbon dioxide. Pounds et al. (1999) hypothesized that the effect of increased tropical sea surface temperature is similar in nature to GCM simulations of surface warming resulting from doubled atmospheric carbon dioxide (Still et al., 1999), namely increase in cloud base height. Still et al. (1999) suggested further research using mesoscale models that better resolve the local topography and land use change.

Lawton et al. (2001) suggested that, through the alteration of surface heat and moisture transfer, deforestation in the lowlands upwind of elevated areas leads to warming and drying the air masses that are ultimately responsible for orographic cloud formation. Satellite imagery over forested and deforested lowland areas upwind of Monteverde shows distinct differences in formation of fair weather cumulus clouds indicating modification of air masses in this region by land use (Lawton et al., 2001; Nair et al., 2003). Numerical simulations conducted using the Regional Atmospheric Modeling System (RAMS) show convective clouds that form over deforested areas have higher base heights due to a warmer and drier boundary layer (Lawton et al., 2001; Nair et al., 2003). Preliminary numerical simulations of Lawton et al. (2001) also show that lowland deforestation leads to the elevation of orographic cloud bank in the Monteverde region.

The preliminary investigations by Lawton et al. (2001) and Nair et al. (2003) assumed scenarios in which the entire model domain is completely forested (evergreen broadleaf forest) or deforested (pasture) or in which just the lowland areas are deforested. Since deforestation is usually accompanied by changes in hydrological budgets, these studies also assumed different soil water storage in forested and deforested areas and chose values consistent with observations from prior studies. Recently two coordinated research projects have collected a series of ground based observations with the aim of conducting more realistic numerical model experiments in this area. The present study extends the prior works of Lawton et al. (2001), Nair et al. (2003) and uses numerical modeling experiments with realistic specification of atmospheric initial conditions, topography and land use change scenarios to assess the impact of deforestation in upwind areas on the orographic cloud formation in Monteverde, Costa Rica. Section 1 describes the study area and data sets used, section 2 describes the modeling system and methodology while sections 4 and 5 present the results and conclusions.

2 Study Area and Datasets

The present study focuses on the Monteverde cloud forests, located along the crest of Cordillera de Tilarán (Figure 1) in northern Costa Rica. The trade wind flows over Cordillera de Tilarán forcing the formation of frequent and persistent orographic cloud banks along the windward Caribbean slopes. These spill over the crest on to the uppermost Pacific slopes. These cloud banks are responsible for the sustenance of one the most diverse cloud forest ecosystems in the world.

Even though the forest along the Caribbean slopes of the Cordillera de Tilarán remains relatively intact, the forest cover in the lower elevation Caribbean plains of Costa Rica has steadily declined during the past century. Sader and Joyce (1988) estimate a decrease in primary forest cover from 67% of the land area in 1940 to 17% in 1983, while more recently Carlson and Sanchez-Azofiefa (1999) report 29% forest cover for 1991 with deforestation proceeding at an average rate of 4.2%. The estimates of Carlson and

Sanchez-Azofiefa (1999) pertain to the country as a whole; the majority of the remaining forest is montane, while the lowland and premontane regions are largely deforested except in a few National Parks and Wildlife Refuges. The areas upwind of Monteverde, such as the San Carlos and Tortuguero plains, have a long history of deforestation with the exception of Tortuguero National Park located south of the Costa Rica-Nicaragua border.

Various datasets are used to both initialize and validate the Colorado State University Regional Atmospheric Modeling System (RAMS) in the present study. The National Center for Environmental Prediction (NCEP) reanalysis data (*Kalnay et al*., 1996) and rawinsonde observations obtained during the Land Use Cloud Interaction (LUCIE) field experiment are used to derive the initial atmospheric conditions and temporally varying lateral boundary conditions used in the RAMS simulations. During the LUCIE field experiment conducted in northern Costa Rican during March 2003, atmospheric conditions were sampled over several paired forested and deforested sites at 3-hour intervals starting from 0600 Local Time (LT) to 1800 LT using coincident rawinsonde launches.

The United State Geological Survey (USGS) topography data and the University of Maryland global land use categorization (Hansen et al., 2000), both of 1 km spatial resolution, are used to specify terrain and surface vegetation type in RAMS simulations. Leaf Area Index (LAI), a crucial input used by the RAMS surface vegetation parameterization, is specified using 1 km spatial resolution LAI composite maps derived from Moderate Resolution Imaging Spetroradiometer (MODIS) data (Myneni et al., 1997; Knyazikhin et al., 1998) available at eight day intervals. The spatial distribution of surface soil types are specified in the RAMS using the 1° x 1° resolution Food and Agricultural Organization (FAO) soils database. The Geostationary Operational Environmental Satellite (GOES-8) imagery is used to assess the ability of the RAMS to simulate orographic cloud banks. Automated cloud classification algorithm of Nair et al. (1999) is used to identify clouds for comparison to RAMS simulated cloud fields.

3 Methodology

This study uses the RAMS to conduct numerical simulations similar in nature to that those used in prior studies of Lawton et al. (2001) and Nair et al. (2003) with the aim of investigating the hypothesis proposed by prior studies, namely that deforestation in the lowland and premontane regions upwind of the Cordillera de Tilarán affects the nature of orographic cloud banks, especially base heights and spatial extent. Three sets of numerical experiments using RAMS, initiated from exactly same atmospheric conditions and subject to the same temporally varying lateral boundary forcing, are used to simulate orographic cloud formation in the study area during the time period of 1-14 March, 2003 for three land use scenarios: a) pristine conditions, i.e., completely forested, including the lowland and premontane regions; b) current conditions specified using the MODIS land use classification; and c) future scenarios where lowland and premontane regions are completely deforested, but the; mountain tops still remain forested (Figure 2).

3.1 Numerical modeling experiments

The RAMS (Pielke et al., 1992) is a versatile non-hydrostatic numerical modeling system, used for simulating a wide range of atmospheric phenomenon raging from micro scale flow around buildings to synoptic scale features. The RAMS uses finite difference techniques to solve a coupled set of partial differential equations for conservation of mass, momentum, heat, and solid and liquid phases of water on a grid that uses a polar stereographic projection in the horizontal, and a terrain following sigma coordinate system in the vertical (Mahrer and Pielke, 1974). Sophisticated parameterization schemes are available in RAMS to account for complex microphysical processes (Walko et al., 2000), land-atmosphere interactions (Tremback and Kessler, 1985; Walko et al., 2000), atmospheric radiative transfer, subgrid scale turbulence, top and lateral boundary conditions.

The numerical simulations used a nested grid configuration (Figure 2) with a fine grid of 1 km spacing and domain of 62 km x 42 km is nested within a coarser grid of 4 km spacing and covering a domain of 400 km x 160 km. The grids are centered approximately on the Monteverde region (10.25°N, 84.7°W). The inner grid allows simulation of orographic cloud formation at fine spatial resolution, while the outer coarse grid allows propagation of larger scale atmospheric flow through the model domain, and insulates the fine grid from lateral boundary forcing effects. A stretched grid was utilized in the vertical for both grids, with a grid stretch ratio of 1.2, and grid spacing that varied from 20m near the surface to 750m higher up in the atmosphere. The topography within the two grids are shown in Figure 1, and the spatial distribution of land use assumed in the three sets of numerical modeling experiments are shown in Figure 2.

The initial atmospheric conditions and a time series of dynamic and thermodynamic fields used for forcing the lateral boundaries in the numerical simulations are drawn from the NCEP reanalysis pressure grids and rawinsonde profiles obtained during the LUCIE field campaign. A Newtonian relaxation scheme is used nudge the atmospheric conditions along the lateral boundaries of the outer coarse grid towards observations. The variables along the lateral boundaries are adjusted by amounts proportional to the differences between the current model predicted values and the values at the same point given by one of the LUCIE-NCEP analysis fields (available at 6 hour intervals) at a future time, with the proportionality constant given by the inverse of a user specified nudging time scale. The nudging scheme is applied to a border region along the lateral boundaries with a width of five grid points and the strength of the Newtonian forcing term is exponentially decreasing towards the domain interior. The strength of the forcing term is controlled by the nudging time scale, which was specified to be 900s. The Klemp and Wilhelmson (1978) lateral boundary conditions were applied to the coarse grid, allowing disturbances to propagate out of the model domain without strongly reflecting back into the interior.

Based on the values reported in the FAO soil database (FAO 1971-1981, Webb et al., 1992, Gerakis and Baer, 1999), an average value of 2.5m was chosen as the depth of the soil layer. In situ observations from the study area for March of 2003 show soil saturation varying between 10-15%, 10-20% and 25-30% at 20, 50 and 100 cm soil depth for both forested and deforested areas. However, field observations suggest pasture grasses in deforested areas are more stressed during the dry season than are trees, implying that the trees have access to water stored in deeper soil layers. This is consistent with prior studies that showing enhanced access to soil water by deeply rooted forest vegetation compared to more shallowly rooted vegetation in the deforested areas. Nepstad et al. (1994) reports that in eastern Amazonia 75% of all the water extracted during the dry season originates from soil layers below the depth of 2m. In the numerical model experiments, soil moisture at depths between 0 and 1 m is specified to be consistent with the averaged observed values. In order to represent enhanced soil water access by more deeply rooted vegetation, soil saturation is allowed to increase from 0.3 at 1 m depth to 0.8 at 2.5 m depth. This manner of prescribing the soil moisture profile assumes that the forest vegetation has access to deeper soil layers and is thus less water stressed compared to vegetation in deforested areas.

Land use scenarios assumed in the three sets of numerical model simulations are as follows: a) In the pristine scenario, broadly consistent with original distribution of forests (Gomez, 1986; Holdridge, 1967), evergreen broadleaf forest is assigned to deforested areas above 750m on the Pacific slope and the entire Caribbean slope. Deciduous broadleaf forest is assigned to deforested areas below 750 m on the Pacific slopes (Figure 2a); b) The current land use scenario is prescribed using the UMD 1km spatial resolution land use type classification (Figure 2b); and c) The deforested land use scenario assumes that the deforestation extend to 1000m and 1400m on the Caribbean and Pacific slopes of the Cordillera (Figure 2c) respectively.

In the current land use scenario, the spatial distribution of LAI is specified using values from the MODIS derived LAI dataset. The grid points that have the same land use type in all the three scenarios are assigned the current MODIS derived LAI value at that location in all the simulations. In the pristine scenario, the forests that replace the currently deforested areas are assigned LAI values consistent with average values of MODIS derived LAI observed for remnant forest at present. Similarly, the locations that are forested at present but are deforested in the future scenario are assigned the average MODIS derived LAI values presently found over deforested regions.

The explicit microphysical parameterization (Walko et al., 2000), the two stream atmospheric radiative transfer scheme of Harrington et al. (2001), and the horizontal diffusion scheme based on horizontal deformation and vertical diffusion parameterization of Mellor and Yamada (1982) are used in all the simulations. Time steps of 4 seconds and 1 second are used for the coarse and fine grid. Radiation calculations are updated every 300 s.

4 Results

All three simulations were conducted for a 14 day period and were initialized using 1 March 2003, 1200 UTC observations. Results from the simulation of current land use are compared against satellite observations and *in situ* atmospheric observations to assess the performance of RAMS in predicting orographic cloud distribution. The three simulations are then inter-compared to determine the differences in orographic cloud characteristics, especially cloud base height and areal extent, in response to varied land use. The simulations are also used to understand the differences in boundary layer thermodynamic and surface energetics that are responsible for the differences in simulated cloud formation.

4.1 Comparison of simulated cloud distribution for current land use to satellite observations

The ability of RAMS to realistically simulate orographic cloud distributions is evaluated by comparing simulated cloud fields in the 1 km space fine grid to GOES-8 observed cloud distribution at similar spatial resolution. The automated cloud detection algorithm of Nair et al. (1999) is used to detect clouds in GOES-8 imagery acquired at one hour intervals starting at 1215 UTC (6:15 am local time) and ending at 2215 UTC. Comparison is restricted to daytime hours, since detection of low level clouds without visible channel imagery is problematic. Comparison is made between each grid point in the inner fine grid to the corresponding location in the cloud mask generated from the hourly GOES-8 observations. From this comparison the following statistics are derived: 1) Number of grid points for which both observations and RAMS simulation show occurrence of cloud (n), 2) Number of grid points for which RAMS simulation shows cloud but satellite imagery does not (n^+), and 3) Number of grid points where cloud occurs in satellite imagery but not in the RAMS simulation (n^-). An accuracy measure (A) is computed from these statistics using the following expression:

$$A = \frac{n}{n + n^+ + n^-} \times 100\,\% \tag{1}$$

Accuracy measures computed from a set of 142 comparisons show wide range of values from 0 to 87%. Visual inspection suggest that the low accuracy values occur under observed conditions of low cloud cover in which the model failed to simulate cloud, or formed cloud at different locations than those observed. Most frequently, model simulations show accuracy values raging from 20% to 70%, with 102 out of the 142 comparisons (72%) showing values greater than 40%. Visual comparison between numerically simulated cloud field and satellite observations shows very good correspondence, especially in the location of the lee edge of the orographic cloud bank (Figure 3). Based on the accuracy measure, out of the 14 days of simulations, six days, 2, 3, 4, 5, 12 and 13 March, 2003 exhibit the best performance. Discussion from this point on is restricted to these days for which the simulations best resembled the observed cloudiness.

4.2 Comparison of temperature and dewpoint in the current land use simulation to LUCIE observations

Boundary layer temperature and dewpoint observations (restricted to days discussed in section 4.1) from LUCIE radiosonde measurements show good correlation over areas upwind of Monteverde with corresponding values from simulation assuming current land use. Air masses upwind of Monteverde are responsible for the formation of orographic clouds when forced to flow over the terrain, and thus realistic simulation of boundary layer thermodynamics in these upwind areas is important. Comparisons between observation and model simulations of temperature and dewpoint in the atmosphere below 850 hPa layer show correlation coefficients of 0.94 and 0.78 (n = 253) respectively. Since the lower layers of the atmosphere respond most to surface influences, good correlations between simulated and observed values of temperature and dewpoint in these layers indicate reasonable representation of surface processes by the model. The LUCIE observations are utilized in the analysis of atmospheric fields that force the RAMS lateral boundary conditions, so it might appear that good correlation between the simulation and observations is an artifact of the assimilating the LUCIE derived information. However, note that the Newtonian nudging is applied only to five grid points bordering the lateral boundaries of the outer coarse grid, far removed the inner grid, and the strength of the nudging term decreases exponentially towards the domain interior. Thus within the domain of the inner fine grid atmospheric conditions are determined mainly by the physical processes simulated by the model rather the data assimilation process.

4.3 Impact of land use change on the characteristics of the orographic cloud bank

The RAMS simulations show consistent differences in the characteristics of orographic cloud banks between the three land use scenarios. Cloud cover characteristics were analyzed over the area which would remain forested even in the scenario involving increased future deforestation. These forests are present from 1000m to the mountain tops on the Caribbean slope and from 1400m to the crest of the mountain on the Pacific slope. At these sites, simulations show a decrease in the areal extent of orographic cloud present at the surface in response to lowland and premontane deforestation and the amount of decrease is proportional to the extent of deforestation (Figure 4a, 4b). Comparisons show a diurnal modulation of the differences in areal extent of at-surface orographic cloud cover. During the morning hours the at-surface areal extent of orographic clouds is very similar in the three simulations, and exhibits a steadily decreasing trend as the morning progresses. During the afternoon hours, at-surface areal extent shows increasing trends in all the three simulations (Figure 4a), but shows differences in absolute value of areal extent (Figure 4b). The afternoon, at-surface areal extent of orographic clouds is highest for the forested scenario, followed successively by the current and deforested scenarios (Figure 4a).

Base heights of orographic cloud banks, as well, show differ among the three simulations. Vertical cross sections of the RAMS simulated orographic cloud bank show it extending to lower altitudes both along the Caribbean and Pacific slopes for the pristine land use scenario (Figure 5a) compared to current (Figure 5b) and deforested (Figure 5c) scenarios. Averaged cloud base heights exhibit a pattern very similar to that observed for at-the-surface orographic cloud cover. Cloud base heights in all the simulations increase steadily during daytime reaching a maximum at 1300 LST and then decrease later in the day (Figure 6a). Averaged cloud base heights in the three simulations are similar earlier in the day but start to differ at about 1130 LST. The largest differences in cloud base heights are found between the deforested and forested simulations; the average cloud base height is higher by a maximum of 170m in the deforested simulation (Figure 6b). The next largest differences are found between the deforested and current scenarios; the average cloud base height is higher in the current scenario by maximum values of approximately 120 m. The least differences are found between the current and forested scenarios; the cloud base heights are higher in the current scenario by up to 70 m.

Numerical simulations thus exhibit a consistent pattern in which average orographic cloud base height and the daytime areal extent of the higher elevation, at-the-ground cloud cover both show declines proportional to deforestation in the lowlands and premontane areas. Diurnal evolution of Lifting Condensation Level (LCL), a surrogate for cloud base height computed from a series of atmospheric profiles measured at 6, 12, 3 and 6 LST over paired forested and deforested sites during LUCIE, shows patterns very similar to averaged evolution of cloud base heights in the pristine and deforested scenarios. Note that direct comparison between LCL derived from the soundings and average model simulated cloud base is not possible, since the latter is an average computed over an area with significant variations in terrain. Elevated terrain restricts the minimum possible cloud base height at a location to be greater than or equal to the surface elevation. However it is valid to compare the trends in LCL and the mean domain averaged cloud base heights. Like average cloud base heights in the pristine and deforested scenarios, LCL is similar over both forested and deforested sites earlier during the day, but starts to differ at 1200 LST with the values being higher over deforested areas (Figure 7). A maximum in LCL is observed at 1500 LST, but the radiosonde measurements were made at 3 hour intervals and hence in reality the maximum value may have been achieved at an earlier hour. Later in the day, LCL starts to decrease over both forested and deforested sites, with the LCL still lower over the forest compared to deforested site.

4.4 Diurnal evolution of surface temperature, dewpoint and energy fluxes

Comparison of mean, domain averaged surface temperature, dewpoint and energy fluxes from the simulations assuming the three different land use scenarios show significant differences in diurnal evolution. The mean averaged surface temperature over the lowlands and premontane regions (1000m and lower) upwind of Monteverde is lowest in the pristine scenario and highest in the deforested scenario (Figure 8a). Maximum difference in mean domain averaged surface temperature between the pristine and deforested scenario, and between the pristine and current scenario are approximately -1.1 and -0.9 K respectively. The mean domain averaged surface dewpoint temperature over the lowlands and premontane regions upwind of Monteverde is highest in the pristine scenario and lowest in the deforested scenario (Figure 8b). The maximum differences between pristine and deforested scenarios, and between the pristine and current scenarios are approximately 1.2 and 1.0 K respectively. Thus deforestation in the lowlands and premontane regions causes the air masses over these areas to be hotter and drier, with the degree of modification proportional to the amount of deforestation.

These results are due to the impact of deforestation on surface energy budgets. Sensible heat fluxes are significantly higher in both current and future land use scenarios compared to the pristine scenario (Figure 8c). Maximum differences in mean domain averaged sensible heat fluxes of approximately -100 Wm^{-2} and -85 Wm^{-2} occur between pristine and future scenarios, and between pristine and current scenario respectively. As expected, latent heat fluxes show a pattern opposite to that of sensible heat fluxes and are significantly higher in the pristine scenario compared to current and future scenarios (Figure 8d). Maximum differences in mean, domain averaged latent heat fluxes of approximately 100 Wm^{-2} and 15 Wm^{-2} are found between pristine and future, and between pristine and current scenarios respectively. Differences in diurnal variation of surface energy fluxes show that enhanced day time transpiration over forested areas are responsible for cooler and moister air over these regions.

5 Conclusions

Recent studies suggest that changes in distributions of dry season mist in at Monteverde in northern Costa Rica have contributed to population crashes and shift of species ranges to higher elevations (Pounds et al., 1999). There could be fewer misty dry season days because of higher bases of the orographic cloud banks (Pounds et al., 1999) resulting from large scale changes in climate (Still et al., 1999). Lawton et al. (2001) and Nair et al. (2003) proposed that changes in land use could also impact formation of orographic clouds, and that deforestation in areas upwind leads to increased orographic cloud base height. The present study extends the work of Lawton et al. (2001) and Nair et al. (2003) through RAMS numerical simulations utilizing realistic atmospheric conditions, topography, land use scenarios and validation against observations.

The RAMS simulations assuming current land use conditions validate the performance of the modeling system. Model simulated boundary layer temperatures, dewpoint temperatures, and orographic cloud characteristics agree well with *in situ* radiosonde measurements over both forested and deforested sites and with GOES-8 satellite observations. RAMS simulations exploring the impact of pristine, current and future land use scenarios in on orographic cloud characteristics in the Monteverde region show that the base height of the orographic cloud banks increases, and areal extent of at-the-surface cloudiness thus decreases, in response to increased deforestation in the upwind locations. Analysis of surface temperatures, dewpoint temperatures, sensible heat fluxes and latent heat fluxes in the premontane and lowland areas show that this is due to warmer and drier air masses forming over deforested areas than over forested ones. These results are consistent with the LCL values calculated from rawinsonde data, which show that throughout the diurnal course of variation the LCL above deforested areas is higher than over forested ones.

The above described findings are also consistent with results from prior studies of Stull et al. (xx) Golaz et al. (2001) and Jeffery et al. (2001) which all show modulation of cloud base heights by land surface processes. The results from the study of Van der Molen (2000), reporting a decrease in orographic cloud base height in response to upwind deforestation, may appear contradictory to the present findings. However, note that the land use change considered in the study by Van der Molen (2000) is different in nature compared to the one considered in the present study. Van der Molen (2000) examined the impact of replacing lower elevation wetland forest in Puerto Rican lowlands by well watered pastures which transpired 14% more than the replaced forests. Thus the land use changes considered by Van der Molen (2000) led to a decrease in the Bowen ratio, while the land use changes considered in the present study led to increase in Bowen ratio. Even though direct measurements of energy fluxes are lacking over paired forest-deforested sites in Costa Rica, there are several other indications that the nature of deforestation in this region leads to an increase in Bowen ratio. Diurnal observations of LCL suggest cooler, moister boundary layer over forested locations. Nair et al. (2003) notes that patterns of cloud formation over forested regions in Costa Rica exhibit linear organization opposed to unorganized convection observed over deforested areas. Organized convection over forested areas is indicative of reduced sensible heat fluxes over forests compared to deforested areas (Nair et al., 2003). Measurements of dry season surface energy fluxes over paired forest-deforested sites in Amazonia (Souza et al., 2000) show the same pattern but differences in magnitudes of sensible heat fluxes that are significantly larger than those reported in the present study. Since there are no obvious reasons to expect the nature of deforestation in Amazonia and Costa Rica to be drastically different, impact of deforestation on surface energy fluxes simulated by RAMS is reasonable. The RAMS simulated temperature and dewpoint temperature profiles compare well to several *in situ* radiosonde measurements over paired forest-deforested sites which is also another indication of satisfactory model performance. However, direct measurements of dry season surface energy fluxes over paired forest-deforested sites are required to confirm the findings of this study.

This study has important implications for conservation of cloud forest preserves. Conservation efforts need to address effects of remote land use changes on cloud forest preserves. The type of changes discussed in this study is also relevant to local hydrology in the vicinity of cloud forests. Since, at several cloud forest sites, horizontal precipitation accounts for a significant proportion of the total precipitation, changes in orographic cloud characteristics has important consequences to local water resources. Quantification of such impacts will provide economic incentives to decision makers for conserving cloud forest ecosystems.

REFERENCES

Bruijnzeel, L. A., 2004: Hydrological functions of tropical forests: not seeing the soil for the trees?, Agriculture Ecosystems and Environment, 104, 185-228.

Carlson, T. N and G. A Sanchez-Azofeifa, 1999: Satellite Remote Sensing of Land Use Changes in and around San Jose, Costa Rica, Rem. Sens. Env., 70, 247-256.

Food and Agriculture Organization - United Nations Educational, Scientific, and Cultural Organization (FAO-UNESCO), 1971-1981, Soil Map of the World, 1:5,000,000, Volumes II-X. UNESCO, Paris, France.

Freedman, J. M., D. R. Fitzjarrald, K. E. Moore, R. K. Sakai, 2001: Boundary Layer Clouds and Vegetation–Atmosphere Feedbacks, J. Climate,14,180-197.

Gerakis, A., and B. Baer, 1999: A computer program for soil textural classification, Soil Science Society of America Journal, 63, 807-808.

Golaz, J.-C., H. Jiang, and W.R. Cotton, 2001:A large-eddy simulation study of cumulus clouds over land and sensitivity to soil moisture.*Atmos. Res.*, **59-60**, 373-392.

Gomez, L. D., 1986: Vegetacion de Costa Rica, Editorial Universidad Estatal a Distancia, San Jose, Costa Rica.

Hansen, M. C., R. S. DeFries and J. R. G. Townshend and R. Sohlberg, Global land cover classification at the 1km spatial resolution using a classification tree approach, Int. J. Remote Sens., 21, 1331-1364, 2000.

Harrington, J. Y., and P. Q. Olsson, 2001: A Method for the Parameterization of Cloud Optical Properties in Bulk and Bin Microphysical Models: Implications for Arctic Cloudy Boundary Layers, Atmos. Res., 57, 51-80.

Holdridge, L. R., 1967: Life Zone Ecology (revised edition) Tropical Science Center, San Jose, Costa Rica.

Kalnay, E., M. Kanamitsu, R. Kistler, W. Collins, D. Deaven, L. Handin, M. Iredell, S. Saha, G. White, J. Woollen,Y. Zhu, M. Chelliah, W. Ebisuzaki, W. Higgins, J. Janowiak, K. C. Mo, C. Ropelewski, J. Wang, A. Leetmaa, R. Renolds, R. Jenne, and D. Joseph, 1996: The NCEP / NCAR 40-year Reanalysis Project. Bull. Amer. Meteor. Soc., 77, 437-471.

Klemp, J. B. and R. B. Wilhelmson, 1978: The simulation of three-dimensional convective storm dynamics. J. Atmos. Sci., 35, 1070-1096.

Knyazikhin, Y., J. V. Martonchik, R. B. Myneni, D. J. Diner, and S. W. Running, 1998: Synergistic algorithm for estimating vegetation canopy leaf area index and fraction of absorbed photosynthetically active radiation from MODIS and MISR data, J. Geophys. Res., 103, 32257-32275.

LaVal, R. 2004: Impact of global warming and locally changing climate on tropical cloud forest bats, J. Mammalogy, 85, DOI: 10.1644/BWG-016.

Lawton, R. O., U. S. Nair, R. A. Pielke, R. M. Welch, 2001: Climatic impact of tropical lowland deforestation on nearby montane cloud forests. *Science*, **294**, 584-587.

Mahrer, Y., and R. A. Pielke, 1975: A numerical study of air flow over mountains using the two-dimensional version of the University of Virginia mesoscale model, J. Atmos. Sci., 32, 2144-2155.

Mellor G. L., Yamada T., 1982: Development of a turbulence closure model for geophysical fluid problems, Rev. Geophys., 20, 851-875.

Myneni, R. B., R. R. Nemani, and S. W. Running, 1997: Estimation of global leaf area index and absorbed PAR using radiative transfer model, IEEE Trans. Geosci. Remote Sens, 35, 1380-1393.

Nair U. S., J. A. Rushing, R. Ramachandran, K. S. Kuo, R. M. Welch and S. J. Graves, 1999: Detection of cumulus cloud fields in satellite imagery. Earth Observing Systems IV, William L. Barnes, Editor, Proceedings of SPIE, 3750, 345-355.

Nair U. S., R. O. Lawton, R. M. Welch, R. A. Pielke.Sr., 2003: Impact of land use on tropical montane cloud forests: Sensitivity of cumulus cloud field characteristics to lowland deforestation., *J. Geophys. Res*., **108**, NO. D7, 4206, doi:10.1029/2001JD001135.

Nepstad, D. C., C. R. de Carvalho, E. A. Davidson, P. H. Jipp, P. A. Lefebvre, G. H. Negreiros, E. D. da Silva, T. A. Stone, S. E. Trumbore, S. Vieira, 1994, The role of deep roots in the hydrological and carbon cycles of Amazonian forests and pastures, Nature, 372, 666-669.

Pielke, R. A, W. R. Cotton, R. L. Walko, C. J. Tremback, W. A. Lyons, L. D. Grasso, M. E. Nicholls, M. D. Moran, D. A. Wesley, T. J. Lee, and J. H. Copeland, 1992: A comprehensive meteorological modeling system – RAMS, Meteor. Atmos. Phys., 49, 69-91.

Pounds, A. J., M. P. L. Fogden and J. H. Campbell, 1999: Biological response to climate change on tropical mountain. *Nature*, **389**, 611-614.

Sader, S. A. and A. T. Joyce, 1988: Deforestation rates and trends in Costa Rica, 1940 to 1983. Biotropica 20, 11-19.

Schrieber, K., Stull, R. and Zhang, Q., 1996: Distributions of surface-layer buoyancy vs. lifting condensation level over a heterogeneous land surface. *J. Atmos. Sci.*, **53**, 1086-1107.

Souza, E. P., N. O. Rennó, M. A. F. Silva Dias, 2000: Convective Circulations Induced by Surface Heterogeneities. *J. Atmos. Sci:*, **57**, 2915–2922.

Still, C. J., Foster P. N. and Schneider S. H., 1999: Simulating the effects of climate change on tropical montane cloud forests. *Nature*, **389**, 608-610.

Tremback, C. J., Kessler, R., A surface temperature and moisture parameterization for use in mesoscale numerical models, 1985: Proceedings of 7th AMS Conference on Numerical Weather Prediction. June 17-20. Montreal, Quebec, Canada, Amer. Meteor. Soc., Boston, 355-358.

Van der Molen, M. K., 2002: Meteorological impacts of land use change in maritime tropics, PhD, Thesis, Vrije Universiteit, Amsterdam, The Netherlands, pg 262.

Webb, R. W., C. E. Rosenzweig, and E. R. Levine, 1992: A global data set of soil particle size properties, NASA Techical Memorandum 4286, 1992.

Walko, R.L., L. E. Band, J. Baron, T.G.F. Kittel, R. Lammers, T.J. Lee, D.S. Ojima, R.A. Pielke, C. Taylor, C. Tague, C.J. Tremback, and P.L. Vidale, 2000: Coupled atmosphere-biophysics-hydrology models for environmental modeling, J. Appl. Meteor., 39, 931-944.

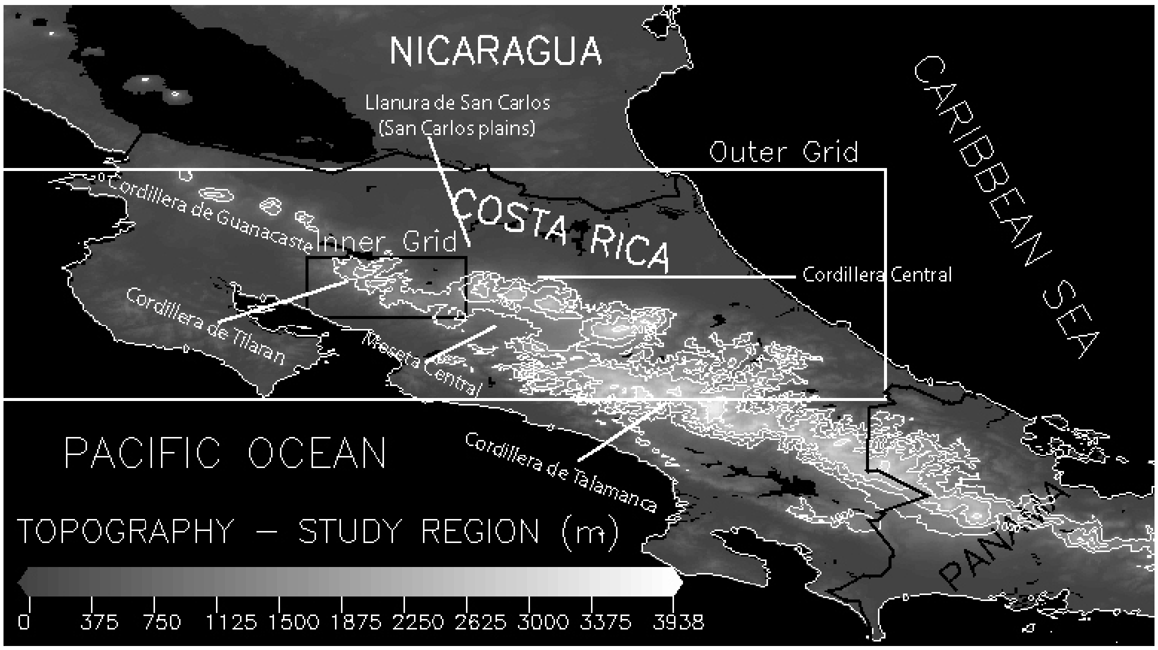

Figure 1 Topography, major mountains, water bodies and model domain referred to in the text. Note the location of outer and inner grids of the model domains with respect to the major mountain ranges and the water bodies. The Cordillera de Tilaran is at the center of the inner grid. The outer grid extends from the Caribbean Sea in the east to the Pacific Ocean in the west.

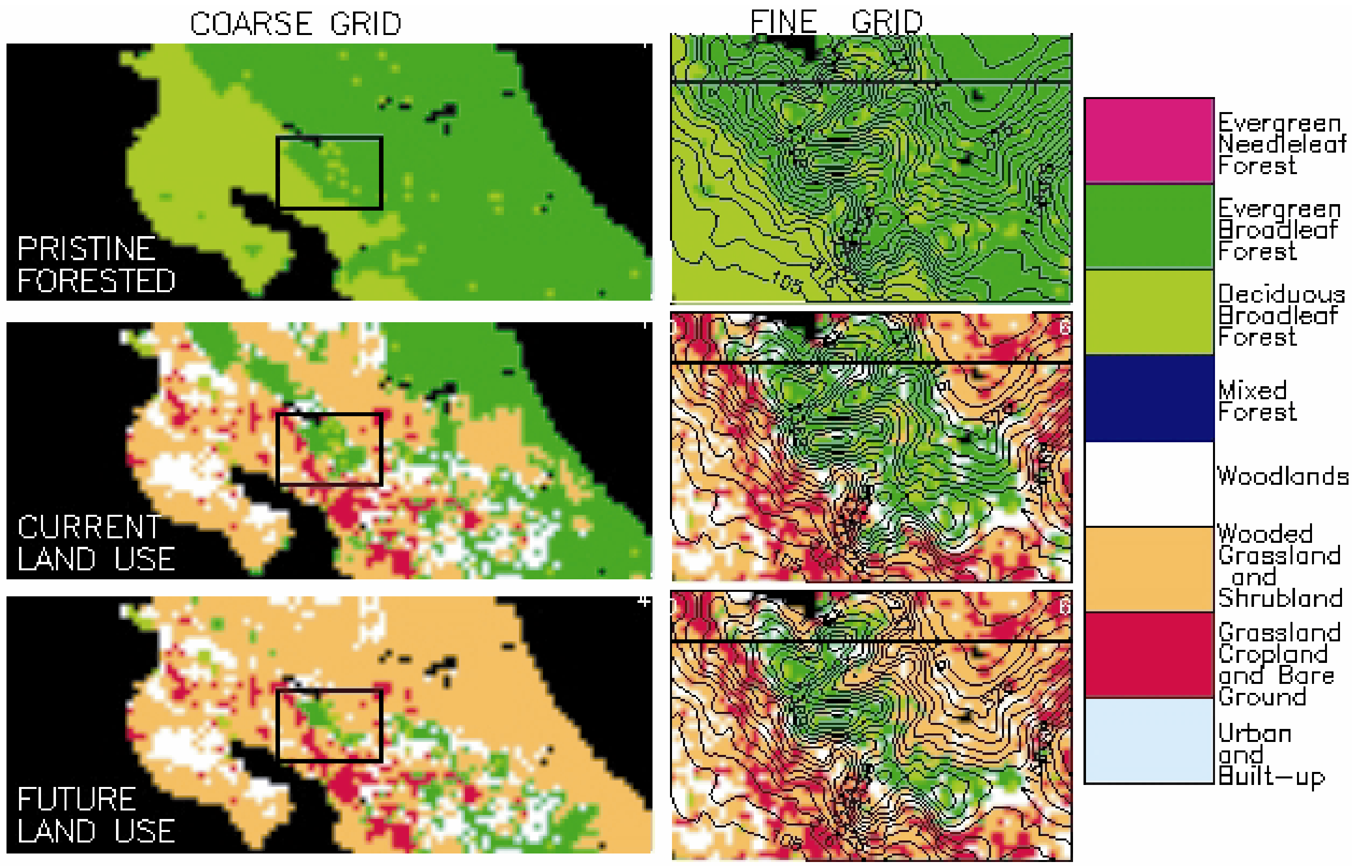

Figure 2

Outer coarse grid (left side panel) and inner fine grid (right side panel) for the three model simulations: Completely forested; current conditions; and only lowland regions deforested. Forested scenario had evergreen broadleaf forests on the wetter Atlantic and deciduous broadleaf forests on the drier Pacific side. In the lowland deforestation scenario, deforestation is assumed to progress till 1000m on the Atlantic side and 1400m on the Pacific side. The Pacific side currently is mostly deforested.

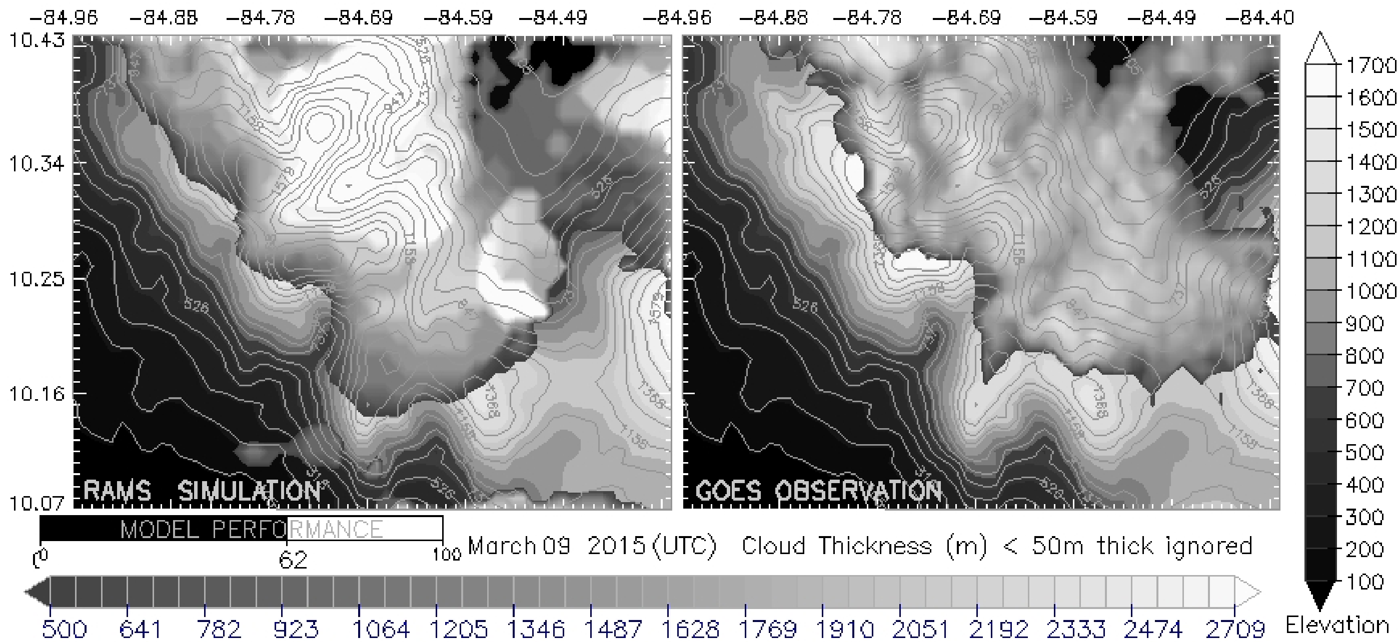

Figure 3. Example of model performance comparison with observed GOES clouds on March 9, 2015 UTC (1415 LT). Left panel shows the RAMS simulated clouds, color coded on the basis of the simulated cloud thickness (horizontal color bar). Right panel shows the GOES observed clouds. The color is the actual brightness values observed. Vertical color bar is associated with topography. In both the panels, the locations where there is no cloud, the topography is visible and the color scheme is that of the vertical color bar. In this particular case the model has 62% accuracy in simulating the clouds.

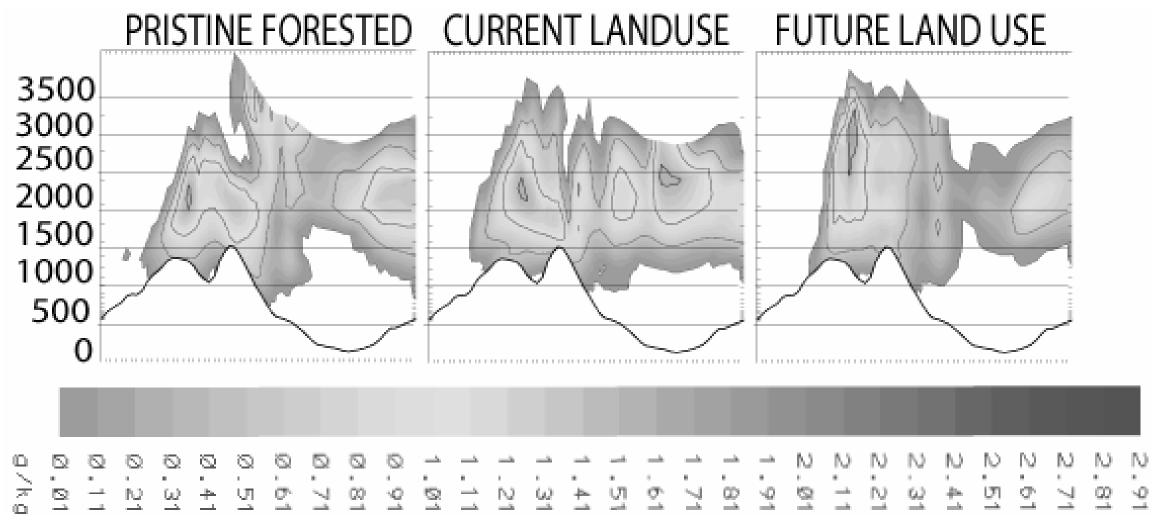

Figure 4 Y-Z cross section plots (along the line Figure 2 fine grid) for the three model scenarios at 1430 LT. Clouds reach the lowest elevations for the pristine forested scenario and the highest for the deforested scenario.

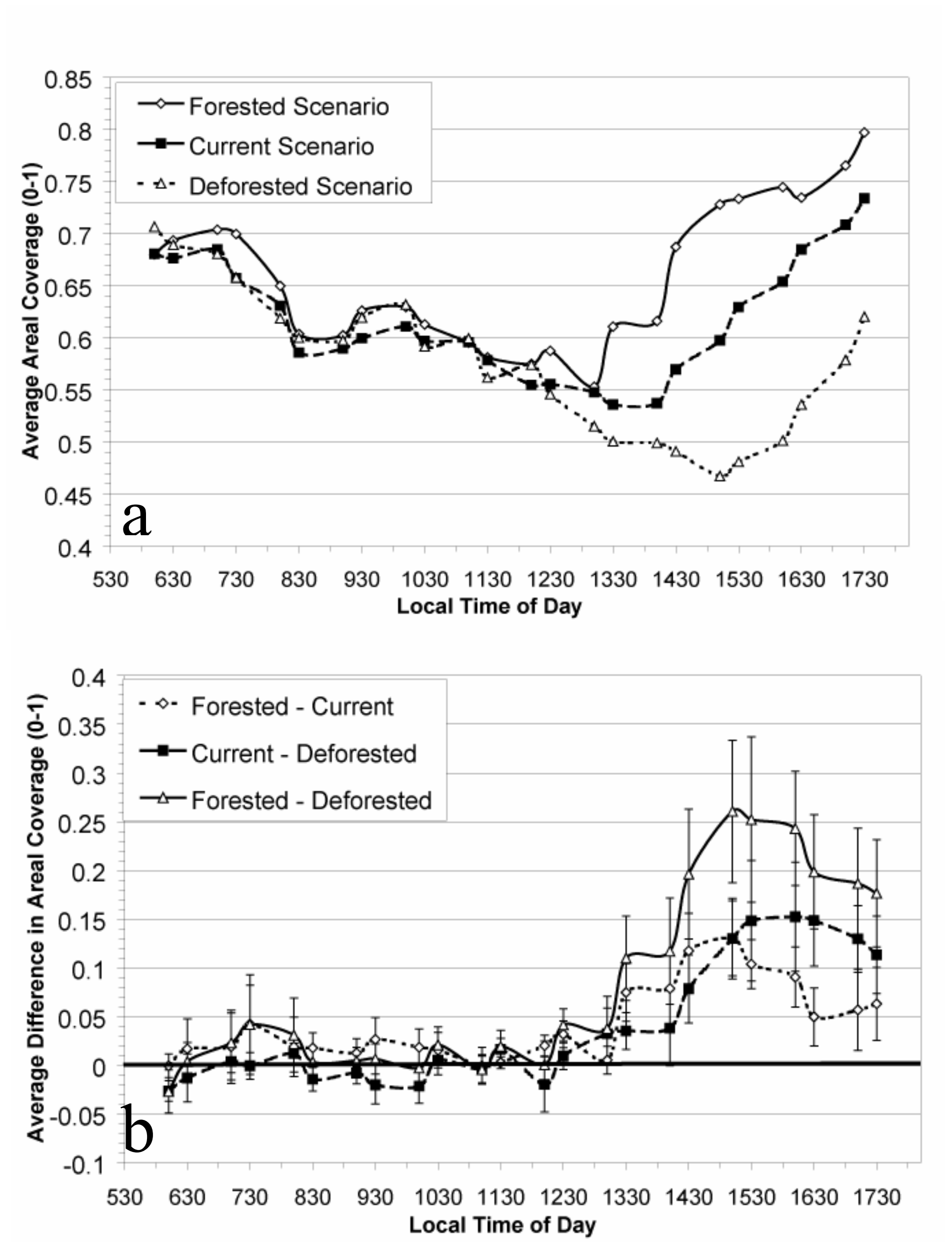

Figure 5 (a) Diurnal variation of the area covered by clouds with bases on the ground (6-day averages). (b) Difference of area covered by clouds with bases on the ground. The bars are the standard error in the estimation of the mean. The total area analyzed for these figures are over the forested areas shown in the inner fine grid for the lowland deforestation scenario.

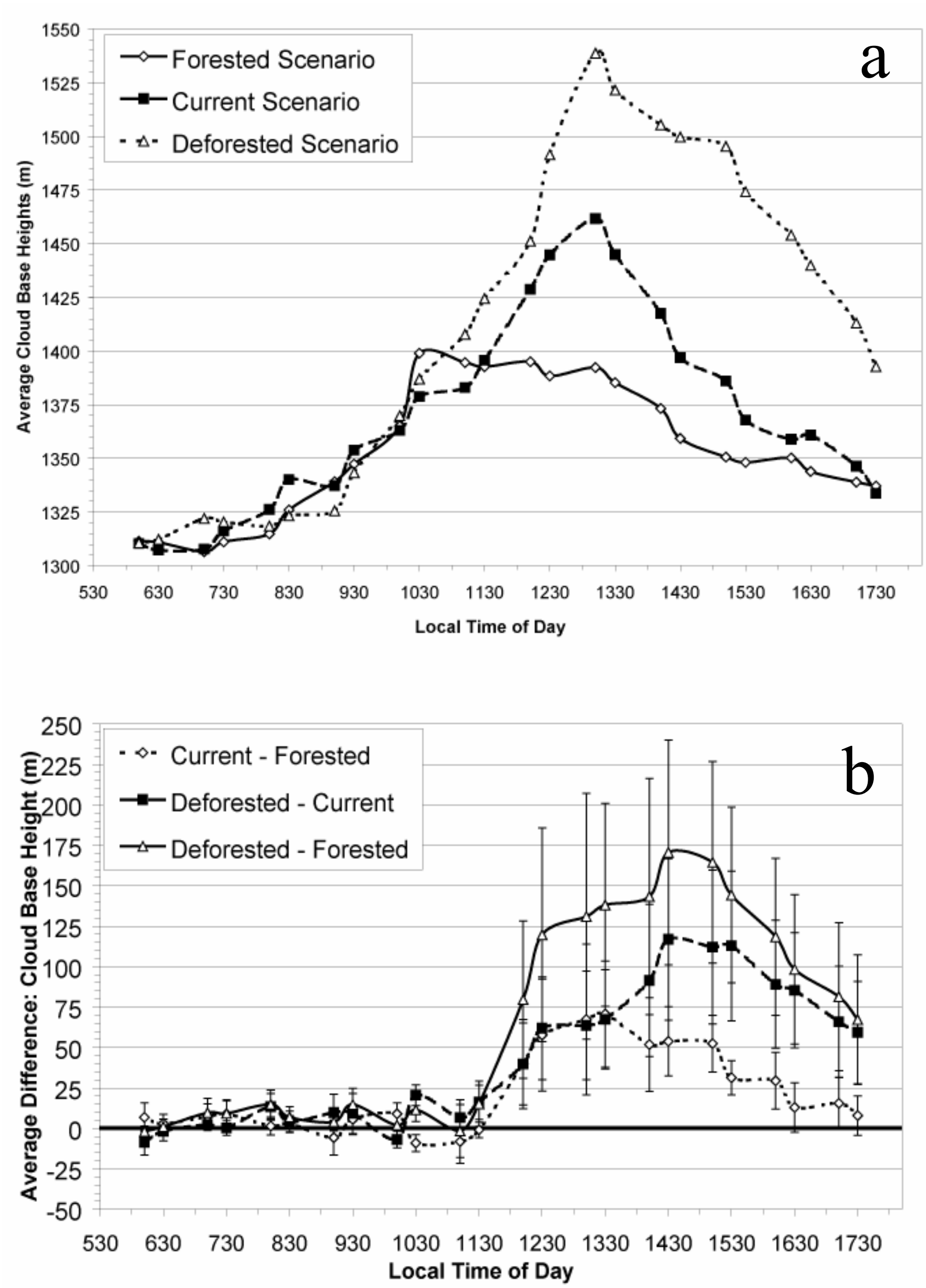

Figure 6 (a) Diurnal variation of 6-day averaged cloud base heights over the remnant cloud forest regions as shown in Figure 2 for the deforestation scenario for the inner fine grid. (b) Difference in cloud base heights over the same region as in (a). The error bars are of the standard error of the mean.

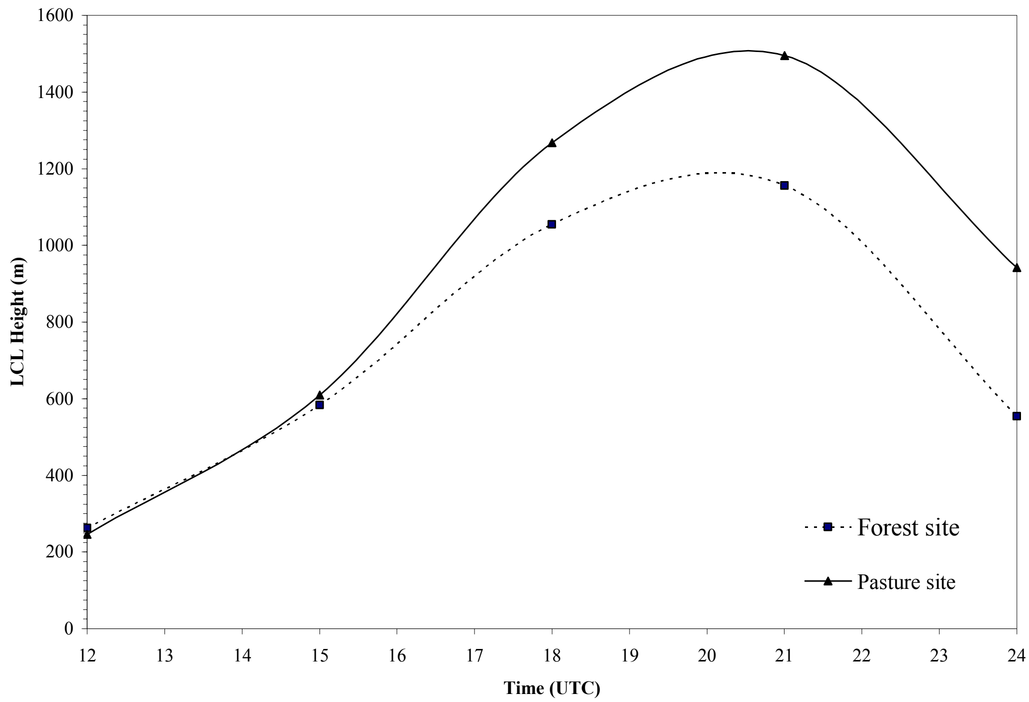

Figure 7. Diurnal variation of average LCL computed from radiosonde measurements obtained over paired forest- pasture sites during March 6-8 of 2003.

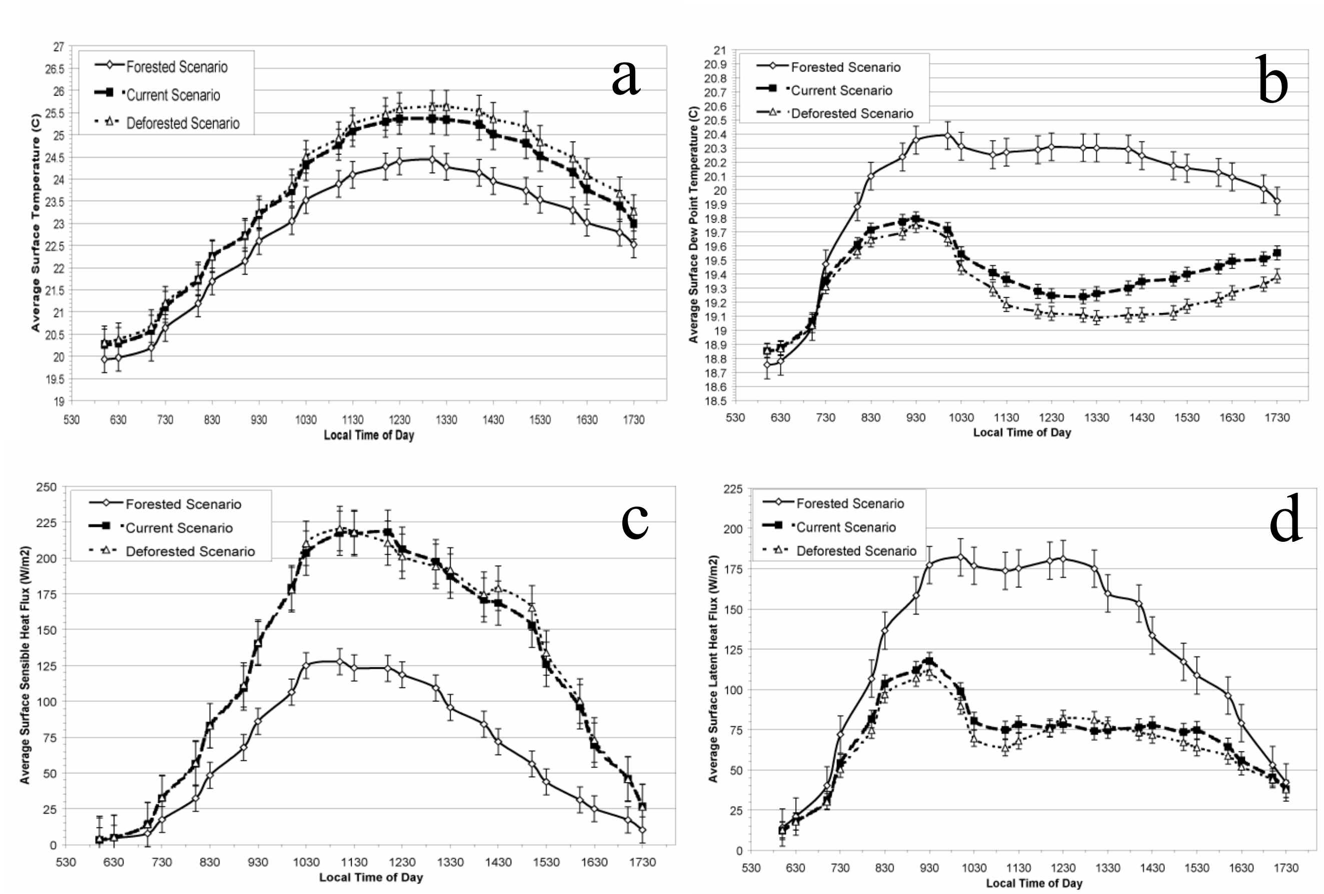

Figure 8 (a) Model lowest level air temperature for the three scenarios. (b) Same as (a) but for dew point temperatures. (c) Same as (a) but for sensible heat flux. (d) Same as (a) but for latent heat flux. The error bars are the standard error of the mean. In each case the domain averaged were the lowland and premontane regions below 1000m.